

Received September 15, 2021; reviewed; accepted September 20, 2021

## Comparative smelting of thermally pretreated electronic waste

Włodzimierz Szczepaniak <sup>1</sup>, Monika Zabłocka - Malicka <sup>2</sup>, Agnieszka Gurgul <sup>1</sup>, Anna Leśniewicz <sup>2</sup>, Katarzyna Ochromowicz <sup>2</sup>

<sup>1</sup> Wrocław University of Science and Technology, Faculty of Environmental Engineering, Wybrzeże Wyspiańskiego 27, 50-370 Wrocław, Poland

<sup>2</sup> Wrocław University of Science and Technology, Faculty of Chemistry, Wybrzeże Wyspiańskiego 27, 50-370 Wrocław, Poland

Corresponding author: [monika.zablocka-malicka@pwr.edu.pl](mailto:monika.zablocka-malicka@pwr.edu.pl) (M. Zabłocka-Malicka)

**Abstract:** Used electronic inverters were processed thermally to eliminate organic matrix components through oxidative incineration (IN), oxidative steam gasification (SG), and pyrolysis (PY). Such prepared material was melted at 1250°C with sodium/calcium silicate waste glass under reductive and oxidative atmospheres. The highest Cu recovery in the form of a gravitationally separated metallic phase was found for oxidative smelting of the PY sample and reductive smelting of the IN sample. Recovery of precious metals was analyzed, taking Cu recovery as the reference. It was found that the recovery of Pd was better than copper recovery in each experiment, and the recovery of Au was only in the oxidative smelting of the SG sample and reductive smelting of the IN sample. Recovery of Ag and Cu was similar but only for the reductive smelting of the PY and SG samples. It was demonstrated that Cu, as well as Au, Ag, and Pd recovery, substantially depends on the transport of metals through the metal/slag interface.

**Keywords:** electronic waste, precious metals, recycling, incineration, gasification, pyrolysis, smelting

### 1. Introduction

Electronic waste is one of the fastest growing waste stream worldwide due to the rapid economic growth and development of modern technologies. Life-time of electronic equipment decreases with time and growing consumption (Forti et al., 2018), therefore proper management of this stream of waste is an important issue. In 2016, globally 44.7 Mt of e-waste was generated and only 20 % of this amount (8.9 Mt) were documented to be collected and properly recycled (Baldé et al., 2017). It means that the remaining (not documented) 80 % (35.8 Mt) of e-waste could be mixed together with municipal solid waste or recycled under inferior conditions. Because of a growing need for metals and global worries that primary resources may be insufficient to meet the future demands (Elshkaki et al., 2018; Schipper et al., 2018), e-waste could be a potential resource of secondary raw materials, especially copper and precious metals of high economic value (Cayumil et al., 2016; Ventura et al., 2018). In 2016, this value was estimated at 55 billion Euros (Baldé et al., 2017), proving that e-waste can be an important and rich resource of metals. Thus, it is essential to improve and increase the proper recycling of electronic waste, and from the economic point of view, for this purpose, circular economy models should be adopted (Cucchiella et al., 2015). However, sustainable management of electronic waste requires the development of recycling and metal recovery technologies that will meet global environmental regulations. This is because the components of e-waste might contain toxic substances that could pose risk to the environment (Man et al., 2013).

For example, PCBs (Printed Circuit Boards) (Kumari et al., 2016 a; Kumari et al., 2016 b; Zhang and Xu, 2016) which are the subject of many studies on recovering metals from e-waste, are considered the most valuable components of electronic devices due to the precious metals contained. Yet, this type of

waste may also contain heavy metals (e.g., Hg, Pb, Cd) (Khaliq et al., 2014) and organic materials that could harm the environment and humans when not properly treated or if recycling is inadequately controlled (Kaya, 2016). Because of considerable differences in matrix composition and metals' content, used electronics constitute a heterogeneous mass of waste, for which it is difficult to implement a suitable recycling model. Methods of metals extraction from PCBs and subsequent refining techniques can be based on pyrometallurgy (Wang et al., 2017), hydrometallurgy (Iannicelli-Zubiani et al., 2017; Sethurajan et al., 2019), or bioleaching processes (Priya and Hait, 2017), or their combination with specific pretreatment.

Pretreatment is an important step in electronic waste recycling that increases the efficiency of metals recovery and decreases the cost of recycling. Pretreatment of electronic waste includes manual and mechanical disassembly, shredding, crushing, and grinding (Kaya, 2017). The aim of this stage could be size reduction, material separation (e.g. non-ferrous and metal fractions), reduction of nonmetallic fraction, and liberation of metals (e.g. by heat treatment). It is also an important step for sorting different e-waste components e.g., batteries and PCBs that could be processed in the next steps to recover valuable resources.

Regarding PCBs, which are the main focus of this article, metals that are contained in this type of waste could be recovered by chemical, biological, and thermal processes. For hydrometallurgy of PCBs, various leaching and recovery technologies may be used. Leaching processes may have different parameters such as temperature, leaching agent and its concentration, solid-to-liquid ratio, pH, particle size, redox potential, etc. As leaching agents, inorganic acids (i.e., sulfuric, nitric, hydrochloric) are commonly used with the addition of  $H_2O_2$  as an oxidizing reagent. Cyanide leaching is dominant in the gold mining industry and is also used for PCB waste, but it generates plenty of wastewater, has a long production cycle and slow leaching rate. Because of those disadvantages, currently, more attention is paid to non-cyanide processes such as thiourea, sodium or ammonium thiosulfate, and halide (chloride, bromide, iodide) leaching (Zhang et al., 2012 a). The main disadvantages of e-waste leaching are reagent cost, leaching rate, and toxicity. Negative environmental impact is mainly caused by a large amount of contaminated wastewater that is a by-product of these processes. The more cost-effective method that also generates less toxic by-products is bioleaching. Bioleaching is based on the natural ability of microbes to transform solid metallic components into their soluble and extractable forms. Biotechnology is commonly used in metal recovery from ores, but also there is much ongoing research to use various microorganisms to extract metals from electronic waste (de Andrade et al., 2019; Díaz-Martínez et al., 2019) as well as to eliminate plastic components before further treatment (Arshadi et al., 2018). Bioleaching has a lower impact on the environment, but also it is not as effective as chemical leaching. To minimize the environmental impact of metal recovery from e-waste, hybrid technologies have been applied currently. Those technologies integrate chemical processes that are more efficient with a biological approach that has less impact on the environment (Pant et al., 2012).

Pyrometallurgical processing has become a traditional method to recover metals from electronic waste and currently, it is a technology that operates on an industrial scale. Companies such as Xstrata Copper, Aurubis, and Umicore use large smelters to melt crushed electronic scrap at high temperatures to recover non-ferrous and precious metals (Navazo et al., 2014). Smelting of electronic waste may be carried out in different furnaces, depending on the applied technology. In most cases, the wastes entering the reactor are immersed in a molten metal bath with a temperature reaching  $1250^{\circ}C$ . The air in the reactor is enriched with oxygen (Cui and Zhang, 2008). The cost of energy is reduced by the combustion of plastic waste and other flammable materials. Impurities and metals (iron, lead, zinc) are converted into oxides and become fixed in the slag that is processed to recover metals before disposal. The copper and precious metals in the liquid form are then refined and recovered. By smelting electronic waste, it is possible to recover metals with high purity and efficiency, but detailed discussion on environmental issues is missing in the literature. Direct smelting of electronic waste has several disadvantages, like high energy consumption and low selectivity toward individual metals (İşildar et al., 2018), and involves undesirable emissions due to thermal degradation of plastic and epoxy components with flame retardants. This leads to the formation of dioxins which require special treatment before being released into the atmosphere (Man et al., 2013).

In our earlier papers, based on laboratory experiments (Zabłocka-Malicka et al., 2015; Gurgul et al., 2015), the idea of transforming some electronic/electric waste into mineral/metallic products by gasification under steam was presented. The aim of that pretreatment was to completely remove organic components from the waste without the use of air, i.e., to eliminate incineration with direct emission of flue gases to the atmosphere.

Here, the e-waste material was pretreated by means of high-temperature (HT) processes eliminating organic components from PCB, i.e., steam gasification (SG), pyrolysis (PY), and incineration (IN) and then smelted at 1250°C with sodium/calcium silicate waste glass under reductive (RE) or oxidative (OX) atmospheres. The purpose of the current work was to identify differences between products of HT treatment and compare the impact of HT pretreatment of selected PCB waste on metals' recovery after smelting.

## 2. Materials and methods

### 2.1. The waste and flux

Experiments were carried out on samples of notebook screen inverter NRP-25-DEQ18213 (photograph in Table 3). The inverters act as a voltage converter, generating a voltage much higher than the supply voltage. They are used in the backlighting of high-voltage fluorescent lamps in LCD screens. Inverters (FR-4 type multilayer PCBs) were chosen as the test object because they are characterized by the integrated circuit structure typical of electronic waste and by a small amount of built-in components. The mass of a single inverter was about 5.72 g. Dimensions of a single inverter were: 190 (L) x 10(B) x 2(H) mm.

A colorless waste packaging glass was used as a flux. On the basis of literature data, the approximate composition of the glass cullet was assumed as: 71% SiO<sub>2</sub>, 13% Na<sub>2</sub>O, 16% CaO (wt.%) (Federico and Chidiac, 2009).

### 2.2. Thermal pretreatment of inverters

Samples of identical inverters were processed before smelting by incineration, pyrolysis, or steam gasification at 850°C. These processes were performed in a laboratory quartz reactor (of 1200 mm length and 36 mm diameter) sealed with siloxane layers of silicone rubber, placed in a set of tube furnaces. Gases (air or argon) and water (for steam generation) were introduced into the reactor by a thin quartz tube. Producer gases were removed with the Liebig condenser on the opposite side of the reactor – details of the experiments were described elsewhere (Gurgul et al., 2015). After processing, inverters generally preserved the original form but became sensitive to crumbling. Their color was characteristic: incinerated inverters were dark gray, pyrolyzed – black and reddish, gasified under steam were gray and orange (the descriptive characteristic was presented in detail (Gurgul et al., 2015)). Weight losses during thermal treatment were relatively small (Table 2), revealing that the content of polymeric substances (epoxies) in the inverters was low. Qualitative analysis of aqueous condensate from steam gasification revealed that the inverters did not contain bromine (halides).

### 2.3. Smelting

Smelting experiments were carried out in alumina crucibles (2 cm of inner diameter and 8 cm high, ICIMB) in a chamber furnace (Nabertherm N150, Nabertherm GmbH). Solid products from thermal pretreatment processes were mixed with a glass cullet (1.16 < Ø < 3.15 mm) and placed in alumina crucibles. In the case of reductive smelting, the space in the crucible above the mixture was filled with pieces of the graphite rod. The crucible was covered with a thin layer of fire-resistant ceramic mat and placed in a larger alumina crucible (8 cm in diameter and 13 cm high) and filled with charcoal. This crucible was finally covered by a thick layer of the temperature-resistant ceramic mat. In the case of oxidative smelting, the arrangement was identical, except for the graphite and charcoal presence. Samples were heated for 3 hours to 1250°C, held at this temperature for an additional 3 hours, then for several hours freely cooled to ambient temperature. After cooling, the crucibles were broken and the metallic droplets were manually separated. Some of the metallic droplets which exhibited magnetic properties were separated by a permanent magnet.

## 2.4. Chemical analysis

Metallic droplets were digested in aqua regia. In the first step, 5 cm<sup>3</sup> portions of the solution were placed in the beakers, beakers were covered with glass lids, and allowed to stand for 24 hours. If the digestion was not complete, the beakers were additionally slightly heated. Solutions were filtered and diluted to 100 cm<sup>3</sup>.

A Varian SpectrAA 20Plus single-beam flame absorption spectrometer, with a deuterium lamp for background correction, was applied for the determination of Cu, Fe, Zn, Ni, Pb, and Ag content (analytical lines selected for measurements: 324.8 nm, 248.3 nm, 213.9 nm, 232.0 nm, 217.0 nm, 328.1 nm respectively). Working conditions for the instrument operation were selected according to the recommendations of the spectrometer manufacturer.

An Agilent bench-top optical emission spectrometer, model 720, with an axially viewed Ar-ICP and a 5-channel peristaltic pump, with conventional pneumatic sample introducing system, was used for the determination of Au (267.6 nm), Pd (340.5 nm), Sn (283.9 nm), and Sb (206.8 nm) (analytical line selected for measurements:). Operating conditions recommended by the manufacturer were applied.

The concentration of metals in the original non-processed inverters was calculated on the basis of acidic leaching in 2M H<sub>2</sub>SO<sub>4</sub> of incinerated, pyrolyzed and gasified inverters (Szczepaniak et al., 2020), followed by aqua regia digestion of the residue and determination of metals as above.

## 2.5. XRD analysis

A Philips X'PERT diffractometer equipped with a PW 1830 generator, PW 3710 control module, PW 3719 counter, Cu K $\alpha$  radiation lamp ( $\lambda=0.15406$  nm) and Ni filter working at 40 kV and 30 mA was used for XRD analysis. The 2 theta angles ( $2\theta$ ) ranged from 3° to 100° at a scan rate of 0.05° per second. The identification of phases was carried out with reference diffraction records from the Powder Diffraction Files Database (International Centre for Diffraction Data, 1998).

## 3. Results

The average concentration of selected metals in the original inverters (before incineration, pyrolysis, or gasification) is given in Table 1. Because the inverters were identical, the standard deviation in Table 1 reflects typical errors of analytical procedures as well as differences in thermal processing (i.e., incineration, pyrolysis, or gasification). However, the identicalness of inverters for the content of trace metals (precious ones) is only an assumption and some fluctuations of these metals content seem probable.

Weight losses registered during thermal treatment are given in Table 2. It may be noticed that the weight loss during steam gasification was more than twice higher than in incineration or pyrolysis.

Table 1. Average concentration of selected elements in original inverters

metal	Cu	Ni	Zn	Fe	Ag	Au	Pd	Sb	Pb	Sn
wt. %	45.0	2.14	0.42	1.44	0.0078	0.083	0.011	0.012	0.068	1.14
SD*)	0.73	0.48	0.069	1.0	0.0040	0.010	0.0020	0.0058	0.048	0.54

\*) - standard deviation

Table 2. Weight losses during incineration, pyrolysis, and gasification of inverters

process	incineration	pyrolysis	gasification
weight loss	7.39%	7.91%	18.15%

All smelting experiments were performed according to identical procedures. The only difference was the oxygen potential of the studied HT processes. Products of smelting, together with the starting material (waste inverters), are presented in Table 3.

Metallic droplets and ingots were isolated manually from the slag. Some of them were additionally separated by a permanent magnet. Both fractions were analyzed for the content of metals – results are presented in Table 4 and Table 5.

To determine the dominating form of copper in thermally preprocessed inverters, the XRD analysis was performed for areas of inverter samples covered by copper foil and exposed to the gaseous phase during incineration, gasification and pyrolysis. Results of the analysis are presented in Fig. 1.

Table 3. Photographs of thermally pretreated inverters (incinerated, pyrolyzed or gasified - top) and their corresponding products after reductive and oxidative smelting: slag and droplets of metal (down)

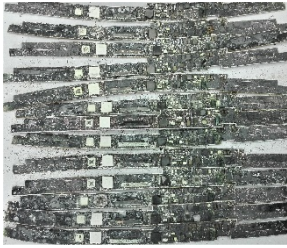
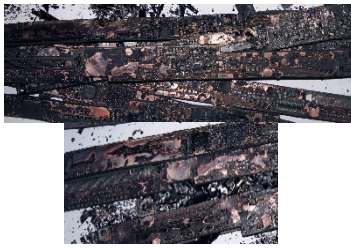









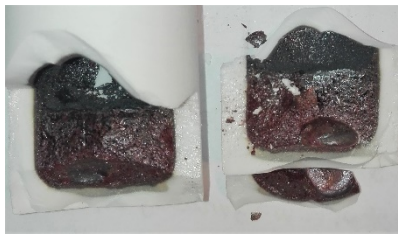


Thermal pretreatment products			
incineration (IN)		pyrolysis (PY)	
		gasification (SG)	
Reductive smelting (RE) products			
slag			
metallic droplets	 RE/IN	 RE/PY	 RE/SG
Oxidative smelting (OX) products			
slag			
metallic droplets	no droplets of metal	 OX/PY	 OX/SG

Table 4. Masses of inverters and other process reagents plus metals' recovery in reductive smelting: TR# - total recovery (in relation to the expected value from the evaluation of data from Table 1, defined as: the mass of the metal recovered [g] / mass of the metal expected [g]), NM\* - in nonmagnetic fraction (NM) and M\* - in metallic fraction (M)

	incineration (RE/IN)			pyrolysis (RE/PY)			gasification (RE/SG)		
mass of original inverter sample (calculated), g	5.8021			6.0991			5.6727		
mass of processed sample used for smelting, g	5.3733			5.6167			4.6431		
mass of flux, g	4.1827			4.1462			4.1542		
mass of separated metal droplets, g	2.0656			0.5265			1.3441		
% of total mass of metals in recovered metallic droplets vs. mass of droplets	88.2			93.7			93.7		
% of separated metals vs. their expected total content	62.4			16.1			44.1		
	NM*)	M*)	TR#)	NM	M	TR#)	NM	M	TR#)
fraction of NM/M	97.05	2.95	-	89.53	10.47	-	20.76	79.24	-
wt. %									
<b>Cu</b>	100.0	0.001	67.25	95.15	4.85	16.71	24.82	75.18	44.74
<b>Ni</b>	94.16	5.84	25.77	68.35	31.65	6.50	0.97	99.03	28.87
<b>Zn</b>	77.91	22.09	0.56	95.89	4.11	0.47	3.36	96.64	28.04
<b>Fe</b>	0.26	99.74	28.35	1.18	98.82	15.83	3.70	96.30	48.60
<b>Pb</b>	79.19	20.81	4.39	88.72	11.28	4.93	21.85	78.15	13.19
<b>Ag</b>	83.54	16.46	36.04	58.48	41.52	20.38	24.98	75.02	41.96
<b>Au</b>	96.53	3.47	95.34	79.30	20.70	3.35	10.16	89.84	17.98
<b>Pd</b>	100.0	0.000	85.84	94.12	5.88	18.37	23.59	76.40	46.41
<b>Sb</b>	19.31	80.69	12.83	79.88	20.12	4.18	43.95	56.05	45.88
<b>Sn</b>	3.17	96.83	6.05	49.23	50.77	16.28	14.39	85.61	50.09

% of recovered Me in NM/M fraction

Table 5. Masses of inverters and other process reagents plus metals' recovery in oxidative smelting: TR# (in relation to the expected value from the evaluation of data from Table 1, defined as: the mass of the metal recovered [g] / mass of the metal expected [g]). There was no magnetic phase.

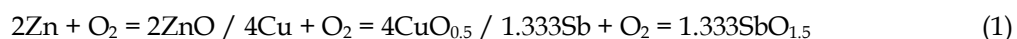
	pyrolysis (OX/PY)	gasification (OX/SG)	
mass of original inverter sample (calculated), g	5.3485	5.6931	
mass of pretreated inverter sample used for smelting, g	4.9254	4.6598	
mass of flux, g	4.4087	3.4584	
mass of separated metal droplets, g	2.1231	0.9446	
% of total mass of metals in recovered metallic droplets vs. mass of droplets	102.4	99.53	
% of separated metals vs. their expected total content	80.7	32.8	
<b>Total Recovery (only nonmagnetic phase, TR#), wt.%</b>			
	Cu	89.56	36.45
	Ni	7.64	1.04
	Zn	11.51	4.97
The reference smelting of the incinerated inverter sample (5.3519 g + 4.1784 of the flux) was also performed –as it was expected there was no droplets of metallic phase; the sintered dark grey/ black product is presented in the photograph in Table 3.	Fe	0.041	0.047
	Pb	3.08	0.91
	Ag	29.76	15.26
	Au	70.01	50.51
	Pd	140.3**	53.34
	Sb	42.44	3.55
	Sn	0.134	0.145

\* above 100% due to analysis uncertainty, \*\*probably due to technical fluctuations of Pd content between inverters

## 4. Discussion

### 4.1. Thermodynamic predictions

Oxygen potential of the redox equilibria. Possible differences between the products of the discussed here processes were related to oxygen potential variations – the oxygen potential defined as  $RT \ln p_{O_2}$ , where  $p_{O_2}$  is the partial pressure of oxygen, for reaction:  $v(\text{red}) + O_2 = v(\text{ox})$ ; for example



$$K = \frac{a_{ox}^v}{a_{red}^v p_{O_2}} \rightarrow \Delta G_r^0 = -RT \ln K = -vRT \ln \left( \frac{a_{ox}}{a_{red}} \right) + RT \ln p_{O_2} \quad (2)$$

where: R – gas constant,  $J \text{ mol}^{-1} \text{ K}^{-1}$ ; T – temperature, K;  $p_{O_2}$  – the ratio oxygen pressure / standard oxygen pressure.

The oxygen potential of steam gasification was discussed in our paper on the PC ISA-card decomposition at the temperature range 800 – 900°C (Zabłocka-Malicka et al., 2018) for three variants.

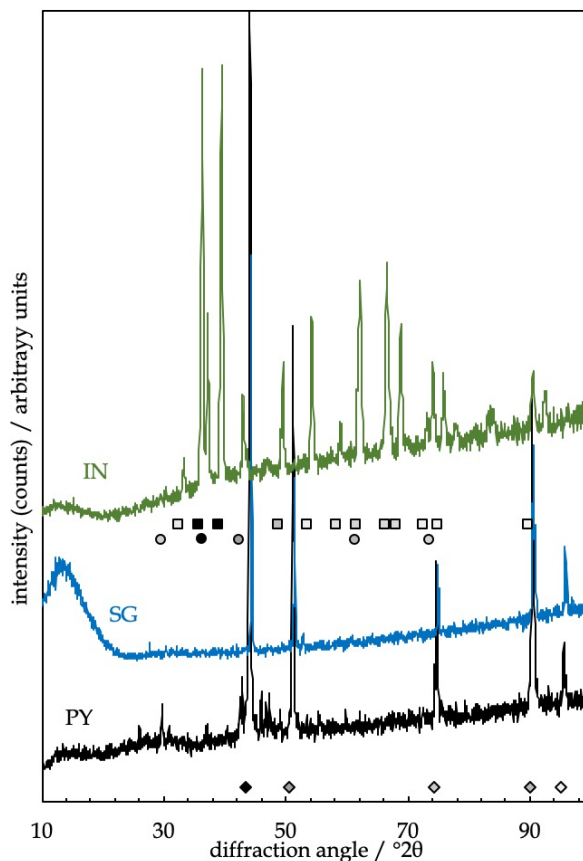


Fig. 1. XRD pattern of Cu-areas in incinerated (IN), gasified (SG) and pyrolyzed (PY) waste inverters. Reference points (International Center for Diffraction Data, 1998):  $\square$  - CuO,  $\circ$  - Cu<sub>2</sub>O,  $\diamond$  - Cu (shadowing represents relative intensity of the reference peaks)

First, equilibration of the gas from the decomposition of the card with steam. Second, gasification of fixed carbon by steam. And third, so-called 'complete gasification' (simultaneous decomposition of the card and gasification of fixed carbon by steam).

During heating, waste components are transformed in a sequence that is specific for the discussed thermal processes. In the final stage of the process of steam gasification, fixed carbon (char) is gasified in the first place, then equilibration of the solid residues with steam takes place. In the pyrolysis, the characteristic was the equilibration of the carbonaceous residue with gas, without steam. The diagrams presented in Fig. 2 are helpful in predicting possible transformations of metals according to thermodynamic equilibria. There are four lines which represent characteristic oxygen potentials for: 1 - air ( $p_{O_2} = 0.21$  bar), 2 - steam ( $p_{O_2} = 4.7 \cdot 10^{-7}$ - $2.3 \cdot 10^{-6}$  bar), 3 - gasification of the carbonaceous residue (char) with steam (HSC Chemistry® Ver. 6.12) ( $p_{O_2} = 1.5 \cdot 10^{-21}$ - $1.5 \cdot 10^{-20}$  bar) and 4 - Boudouard reaction ( $p_{O_2} = 5.9 \cdot 10^{-21}$ - $6.1 \cdot 10^{-20}$  bar). The process of conversion starts from the decomposition of polymeric components and the formation of carbonaceous residue combined with metals and inorganic/mineral fractions. Line 4 seems characteristic for this step because the contact between the atmosphere of the reactor and the inverter core is impossible due to emission of gases from the inverter bulk. This is typical for the pyrolysis process under an inert atmosphere (argon). Except for zinc, other metals should be in a metallic form. However, it should be kept in mind that line 4 represents 'formal' Boudouard equilibrium, calculated for  $p_{CO} + p_{CO_2} = 1$  bar. Recalculating the equilibrium for the partial pressure of oxygen characteristic for the inert gas (Ar,  $p_{O_2} = 1 \cdot 10^{-5}$  bar) results in lowering of the oxygen potential to -642/-606 kJ mol<sup>-1</sup> at 800/900°C, respectively. This means that also the reduction of zinc oxide is possible. When the gaseous emission due to the decomposition of polymeric components is finished, the contact and reaction of the solid residue with the reactor atmosphere are possible. If the steam is the reactor atmosphere, the oxygen potential of the system is represented by line 3 in Fig. 2. It appears that



the reduction potential of the system is even somewhat better. However, the vanishing of the carbonaceous residue (due to the reaction  $C + H_2O = CO + H_2$ ) results in a shift of oxygen potential to line 2, allowing the oxidation of metals, including copper. This discussion concerns the equilibrium of the so-called invariant phase, comprising non-gaseous reagents in the standard state (pure substances), with a gaseous phase which is an ideal solution. This corresponds to the relation  $a_{ox}/a_{red} = 1$  in equation (2). However, it is not a typical situation and the formation of solutions (solid and liquid; metallic alloys in the first place) should be taken into account. It was approximated by an exemplary change of  $a_{ox}/a_{red} = 1$  from 1 to 1000, which may be related to the reduction of a metal from pure oxide to metal in metallic solution (alloy) with a molar fraction of 0.001 (assuming ideality of the system). It is noticed from Fig. 2 that such a change of the component activity does not change the general oxidation/reduction sequence, even if the change of oxygen potentials is relatively significant. It may be therefore concluded that, during pyrolysis and gasification, metals should be reduced (except for zinc) and possibly alloyed. Especially, until the carbonaceous residue is removed. Under steam, they should be oxidized, taking into account the partial pressure of  $H_2$  (calculated below). And during incineration total oxidation should occur.

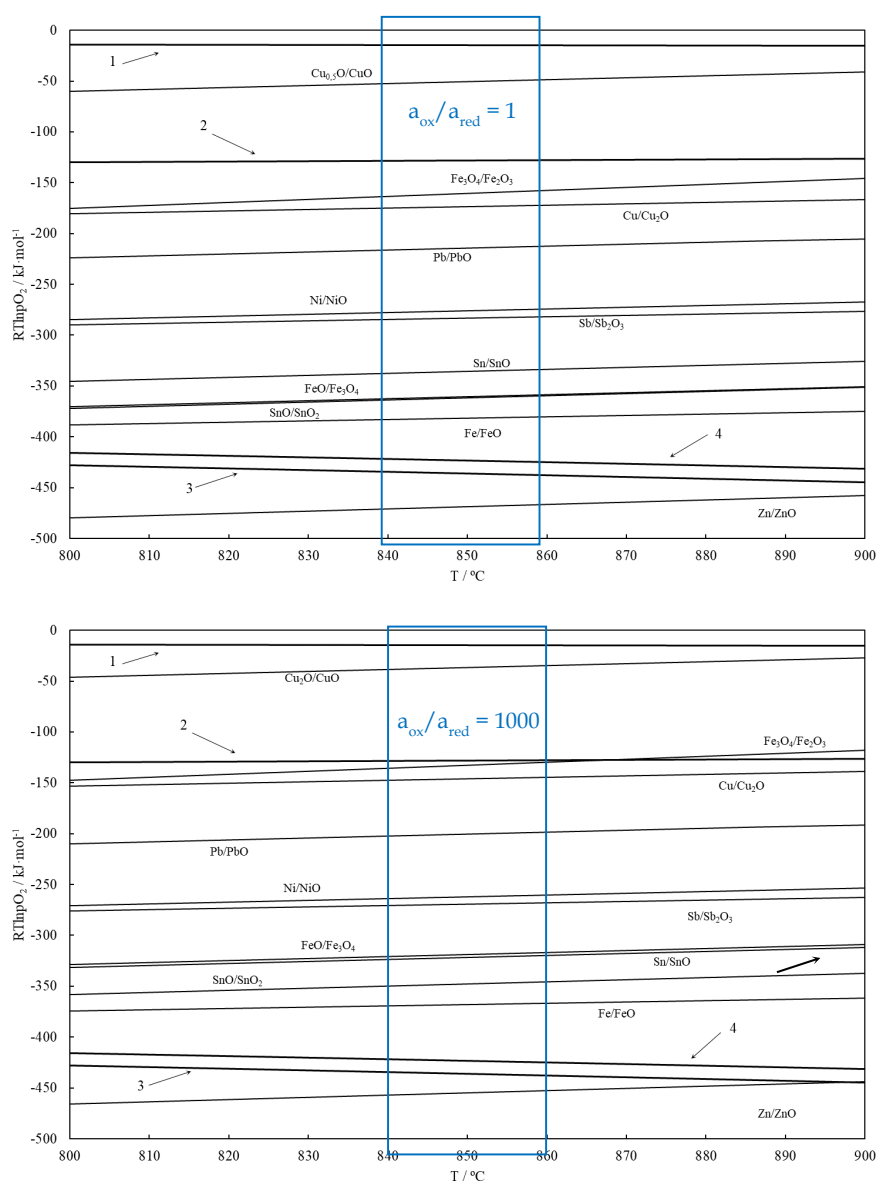


Fig. 2. Oxygen potentials of: (1) - air, (2) - steam, (3) - fixed carbon (char) gasification with steam, (4) -Boudouard reaction. Thin lines represent oxidation equilibria for the investigated non-precious metals (both forms condensed).  $a_{ox}$  - activity of oxidized form,  $a_{red}$  - activity of reduced form. Temperature range of the final equilibration was marked by a rectangle. Calculations were performed with HSC Chemistry® (Ver. 6.12)

*Metal distribution ratios.* Taking into account eq. (2), the equilibrium distribution ratio,  $L_{o/r}$ , may be defined with metal activities in oxidized and reduced forms:

$$\frac{a_{ox}}{a_{red}} = L_{o/r} \rightarrow L_{o/r} = (K \cdot p_{O_2})^{(1/v)} \quad (3)$$

This equation enables evaluating the possible distribution of metals between phases of the system, particularly between the slag and metal phases. Distribution ratios calculated for oxygen potential characteristic for experiments of smelting (1250°C) and thermal pretreatment (850°C) are presented in Table 6. It is important to note that these  $L_{o/r}$ 's values were calculated in the oxide notation as in equation (1).

Table 6. Activity equilibrium distribution ratios,  $L_{o/r}$ , for characteristic oxygen potentials: Boudouard reaction, char gasification (Fig. 2 - line3) and steam (Fig. 2 - line2)

$v^*$	Reaction	$\Delta G_r^0$ , kJ(d)		Lo/r			
		1250°C	850°C	Boudouard reaction		Fig.2 - line3	Fig.2 - line2
				1250 °C	850°C	850°C	850°C
4	Cu / CuO <sub>0.5</sub>	-111.4	-173.5	4.72·10 <sup>-04</sup>	1.25·10 <sup>-03</sup>	8.85·10 <sup>-04</sup>	33.6
2	Zn(l) <sup>(a)</sup> / ZnO	-383.2	-468.7	1.02·10 <sup>-02</sup>	114	5.75	8.28·10 <sup>+07</sup>
2	Pb / PbO	-154.7	-214.3	1.23·10 <sup>-06</sup>	1.38·10 <sup>-05</sup>	6.94·10 <sup>-06</sup>	100
2	Sn / SnO	-269.1	-335.5	1.13·10 <sup>-04</sup>	9.14·10 <sup>-03</sup>	4.59·10 <sup>-03</sup>	6.62·10 <sup>+04</sup>
1.333	Sb / SbO <sub>1.5</sub>	-231.7	-283.5	1.31·10 <sup>-07</sup>	1.33·10 <sup>-05</sup>	4.74·10 <sup>-06</sup>	2.61·10 <sup>+05</sup>
2	Fe / FeO	-328.9	-381.9	1.20·10 <sup>-03</sup>	0.110	5.49·10 <sup>-02</sup>	7.91·10 <sup>+05</sup>
2	Ni / NiO	-207.2	-275.8	9.82·10 <sup>-06</sup>	3.72·10 <sup>-04</sup>	1.87·10 <sup>-04</sup>	2.70·10 <sup>+03</sup>
2	Pd / PdO <sup>(b)</sup>	88.0	7.18	8.50·10 <sup>-11</sup>	9.78·10 <sup>-11</sup>	4.92·10 <sup>-11</sup>	7.09·10 <sup>-04</sup>
4	Ag / AgO <sub>0.5</sub>	115.6	76.4	5.34·10 <sup>-06</sup>	1.55·10 <sup>-06</sup>	1.10·10 <sup>-06</sup>	4.17·10 <sup>-03</sup>
1.333	Au / AuO <sub>1.5</sub> <sup>(c)</sup>	260.2	193.0	2.89·10 <sup>-20</sup>	3.16·10 <sup>-22</sup>	1.12·10 <sup>-22</sup>	6.19·10 <sup>-12</sup>

extrapolated if necessary from: [ZnO(l)](a) - 905°C, [PdO] (b) - 930°C, [Au<sub>2</sub>O<sub>3</sub>] (c) - 230°C

\*for reaction stoichiometry as in equation (1)

The distribution ratios given in Table 6 are representative of the thermodynamically ideal solution. For the real non-ideal solution, activity coefficient,  $\gamma_i$ , should be taken into account, and  $a_i = x_i \cdot \gamma_i$ , where  $x_i$  is the molar fraction of component  $i$ . In the case of diluted solutions, activity coefficients may tremendously affect species activities, therefore they were systematically discussed in the literature (Pickles et al, 2011; Shuva et al., 2016; Yamaguchi, 2018). It is evident that the inverter samples prepared for smelting were highly inhomogeneous. In a general approximation, it might be expected that during the process of smelting at 1250 °C only two phases would be formed – metallic and slag. Taking into account the elemental composition of the non-metallic fraction of the waste PCB (Barazgan et al., 2014) and composition of the glass cullet (Federico and Chidiac, 2009), the approximate composition of the slag (in the base form, without metal oxides) was calculated as 68 wt.% SiO<sub>2</sub>, 21% CaO, 9% Na<sub>2</sub>O and 2% Al<sub>2</sub>O<sub>3</sub>. Assuming that Al<sub>2</sub>O<sub>3</sub> was an amphoteric admixture, the composition of the slag was located in the area of the CaSiO<sub>3</sub> phase-field or, more precisely but uncertain, Na<sub>2</sub>Ca<sub>3</sub>Si<sub>6</sub>O<sub>16</sub> (Zhang et al, 2012 b). According to the phase diagram, the oxide mixture should be liquid at 1250 °C or stay in equilibrium with a small amount of crystalline phase and enable the separation of slag and metal phases. Smelting of processed inverter waste was performed at contrasting oxygen potentials – reductive and oxidative (Table 4 and Table 5). Under chemical equilibrium, metals should be collected in the metallic phase in the reductive smelting, whereas in the oxidative one, they should be oxidized, except for precious ones. However, the data from Table 4 and Table 5 show that the smelting processes were relatively far from equilibrium, typically underway of physicochemical transformations of kinetic nature.

*Oxidation of metals under steam.* As mentioned, under steam and a lack of carbonaceous phase, metals – except for precious ones, should be oxidized. The oxidation reaction, at 850°C, proceeds with the emission of hydrogen at very different partial pressures – Table 7. Regarding the steam volume transferred inside the reactor during the equilibration of the inverter sample gasified with steam, at

850°C, we assumed that all non-precious metals might be potentially oxidized according to the decreasing sequence of H<sub>2</sub> partial pressure in Table 7.

Table 7. Calculated hydrogen pressure for equilibration of metal with steam at 850 °C (for p<sub>H<sub>2</sub>O</sub> = 1 bar)

Reaction	$\Delta G_r^0$ , kJ	pH <sub>2</sub> , bar
2Cu + H <sub>2</sub> O(g) = Cu <sub>2</sub> O + H <sub>2</sub>	99.151	2.45 · 10 <sup>-05</sup>
Zn + H <sub>2</sub> O(g) = ZnO + H <sub>2</sub>	-48.450	179
Pb + H <sub>2</sub> O(g) = PbO + H <sub>2</sub>	78.777	2.17 · 10 <sup>-04</sup>
Sn + H <sub>2</sub> O(g) = SnO + H <sub>2</sub>	18.144	0.143
2Sb + 3H <sub>2</sub> O(g) = Sb <sub>2</sub> O <sub>3</sub> + 3H <sub>2</sub>	133.013	8.67 · 10 <sup>-03</sup>
Fe + H <sub>2</sub> O(g) = FeO + H <sub>2</sub>	-5.026	1.71
Ni + H <sub>2</sub> O(g) = NiO + H <sub>2</sub>	48.021	5.84 · 10 <sup>-03</sup>
Pd + H <sub>2</sub> O(g) = PdO + H <sub>2</sub>	189.502	1.53 · 10 <sup>-09</sup>
2Ag + H <sub>2</sub> O(g) = Ag <sub>2</sub> O + H <sub>2</sub>	224.115	3.77 · 10 <sup>-11</sup>
2Au + 3H <sub>2</sub> O(g) = Au <sub>2</sub> O <sub>3</sub> + 3H <sub>2</sub>	847.342	7.30 · 10 <sup>-14</sup>

extrapolated from: [Au<sub>2</sub>O<sub>3</sub>]<sup>(c)</sup> - 230°C

#### 4.2. Total recovery of metals

First of all, it should be stressed that the goal of the experiments was not to optimize the recovery of the metallic phase, hence the results were not discussed in this context. These experiments only show how pretreatment of raw material (waste) impacts the smelting process. The results were analyzed regarding two types of metal losses – chemical, due to the dissolution of metals in non-metallic phases, and physical (mechanical) - due to the suspension of metal particles in the slag. Both losses define the efficiency of metal recovery (Bellemans et al., 2018).

We assumed that the total content of metals in the inverter samples was equal to the values determined through digestion with aqua regia. Referring to those values, we compared the total recovery of metals for the studied variants of waste HT treatment and smelting – Table 4 and Table 5. Despite the same melting procedure for all samples, very significant differences were found between the levels of metal recovery. In the case of reductive smelting, 62%, 44%, and only 16% of metals were recovered, respectively from incinerated, gasified, and pyrolyzed samples. Oxidative smelting yielded 81% or 33% from pyrolyzed and gasified samples.

#### 4.3. Recovery of copper and precious metals

PCB copper foils were oxidized during oxidative incineration to the mixture of CuO and Cu<sub>2</sub>O (with the domination of CuO) – XRD analysis in Fig. 1. This finding correlates very well with the dark grey / black color of the incinerated sample – cf. Fig. in Table 3. In the case of steam gasification and pyrolysis, copper preserved metallic form, which can be confirmed by identical XRD patterns for both processes. This outcome sticks up for the suggestion from the thermodynamic calculations on stoichiometric limitation of the copper oxidation to Cu<sub>2</sub>O (see Oxidation of metals under steam).

Copper was the dominant metal and played the role of a collector phase for other metallic elements in smelting experiments, therefore its recovery should be discussed separately. It may be noticed from Fig. 3a that the highest copper recovery was for oxidative pyrolysis and reductive incineration, and the lowest one for reductive pyrolysis. The major difference between these experiments was in a radical change of oxygen potential (OX/PY and RE/IN) or the lack of this change (RE/PY). OX/PY was characterized by an initial gradual burning of the carbonaceous residue, and then oxidation of metals, engaging oxygen transport in the slag. In the case of RE/IN, the oxygen potential inside the sample was high at the beginning, because the metals were in oxidized form and the reducer (charcoal) was outside the sample. While in RE/PY, the reducer presence outside and inside the sample caused the stability of

the low oxygen potential throughout the experiment. Thus, in OX/PY and RE/IN experiments, an intense transport of metals between oxide and metallic phases resulted in lowered dynamic interfacial tension (Bellemans et al., 2018) and enhanced metallic droplets coalescence. Instead, in RE/PY test, there was only melting and relatively low mass transport between phases, hindering the coalescence and separation of the metallic phase.

Optimization of copper recovery is a typical pyrometallurgical problem but it was not the aim of our experiments. It seems that the gathering of precious metals by metallic copper separated from the slag in a form of droplets is much more important. This gathering may be discussed as total or relative to copper – Fig. 3 a and b, respectively (relative recovery was defined as % of metal recovery / % of copper recovery). In the relative approach, recovery higher than 1 may be interpreted as a “faster” recovery of the metal in comparison to copper. The differences between the behavior of Pd, Au, and Ag are easy to notice. Recovery of Pd was 1-1.5 times better than Cu and proportional to the total Cu recovery in all experiments. Au recovery appeared approximately 40% better than copper recovery, but only for OX/SG and RE/IN experiments. They were characterized by a relatively long period of high oxygen potential – for RE/IN during HT pretreatment and in the case of OX/SG, after the carbonaceous residue was removed. Domination of the low oxygen potential (reducing process) did not support Au recovery – the sequence of the relative recovery of gold in Fig. 3 b is very characteristic: RE/PY < RE/SG < OX/PY. Contrary to Au, the recovery of Ag seemed supported by low oxygen potential and only for RE/PY and RE/SG silver recovery was comparable to copper recovery. This behavior of copper plus precious metals does not seem to be correlated solely with affinity to oxygen (presented in the form of equilibrium distribution ratios in Table 6) and was probably also related to the spatial allocation in the inverter sample.

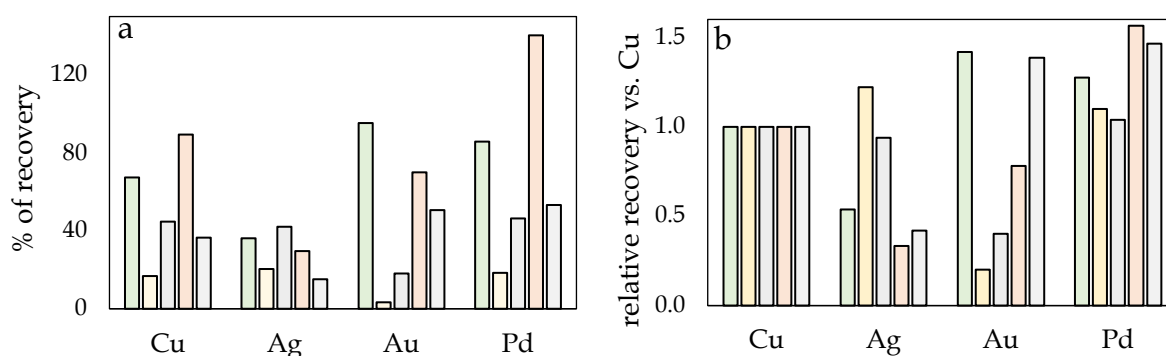


Fig. 3. Total (a) and related to copper (b) recovery of precious metals in smelting experiments (from left): RE/IN, RE/PY, RE/SG, OX/PY and OX/SG (description of symbols in text). Over-recovery of Pd probably due to technical fluctuations of the metal content between inverters

#### 4.4. Recovery of non-precious metals

This group comprised two subgroups – ferrous (Fe, Ni) and non-ferrous (Zn, Pb, Sn, Sb) metals. Their recovery, total and related to Cu, is presented in Fig. 4. It appeared that the separation efficiency was similar to copper only for Fe and Sn in RE/PY, RE/SG processes, and for Sb in RE/SG process. The recovery of other metals was much lower than that of copper, especially for OX-type (oxidation) experiments. A very characteristic composition of magnetically separated metallic droplets should be also noted – Fig. 5. Copper was close to the detection limit in the magnetic phase from RE/IN experiments, constituting 50% of this phase in RE/PY smelting, and as much as 90% in RE/SG. It is evident that Cu contribution determined the mass of magnetically separated phases – Table 4. It is also characteristic that only Fe was concentrated almost exclusively in the magnetic phase, not Ni.

Generally, the question may be asked which experiments were relatively close to chemical equilibrium and which ones not. The two oxidative experiments (OX/SG and OX/PY) were undoubtedly far from equilibrium and more (OX/SG) or less (OX/PY) advanced oxidation occurred. It seems that this is an argument for the lack of magnetic phase in OX experiments and a very low concentration of Fe in metallic droplets. On the opposite, the RE/PY sample should be relatively closest

to the reductive equilibrium, then RE/SG and possibly RE/IN - at the end of the experiment. Therefore, the characteristic Cu / Fe proportions can be found in RE experiments. It should be also noticed that the recovery of Pb and Zn was very low, well below 20% of the total content (with the one exception of Zn in the RE/SG experiment). This, in turn, may be related to the volatility of these elements, typical in metallurgical processing.

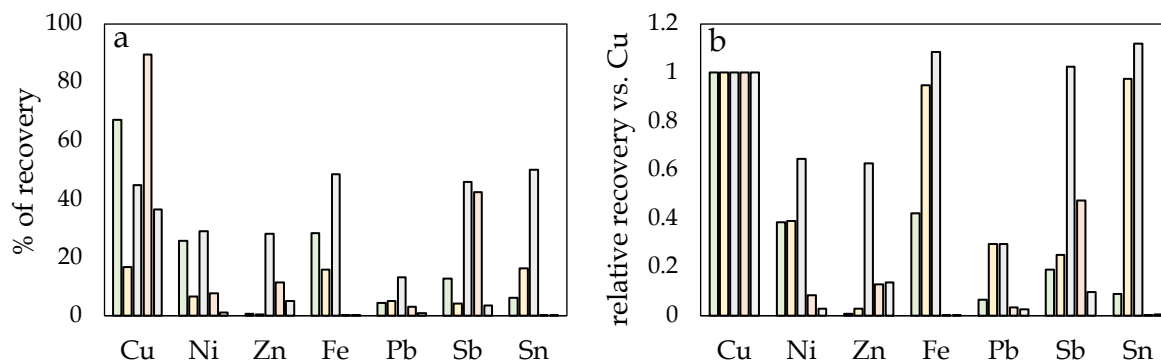


Fig. 4. Total (a) and related to copper (b) recovery of non-precious metals in smelting experiments (from left): RE/IN, RE/PY, RE/SG, OX/PY and OX/SG (description of symbols in text).

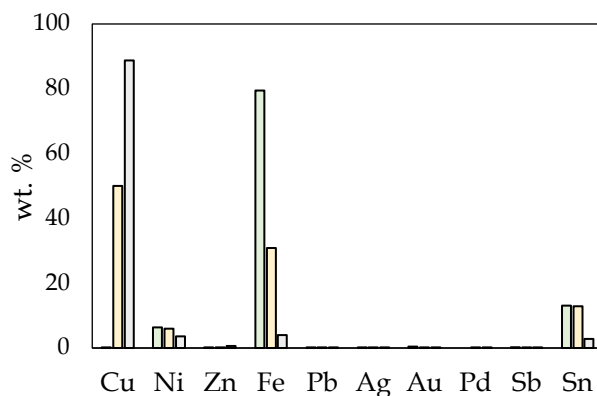


Fig. 5. Composition of magnetically separated metallic droplets in experiments RE/IN (3.0% of separated droplets in total), RE/PY (10.5%), and RE/SG (79.2%). Magnetic phase was not detected in OX/PY and OX/SG experiments.

## 5. Conclusions

Based on the visual inspection of samples and mass loss after HT pretreatment, it may be summarized that: (a) during pyrolysis only volatile matter was released from the inverters, (b) during steam gasification also carbonaceous residue was removed to the gas, and (c) during incineration copper (and other non-precious metals) were completely oxidized. It was evaluated that volatile matter constituted 7.9% of the inverter mass, whereas the carbonaceous residue was 10.2%.

Pre-processing of e-waste inverters by oxidative incineration (IN), oxidative steam gasification (SG), and pyrolysis (PY) had a significant influence on the recovery of metals to the metallic phase:

a) Copper - the dominant metal - was converted into a mixture of copper oxides during incineration. In steam gasification, copper preserved the metallic form due to the low equilibrium partial pressure of  $H_2$ . However, a complete transformation of Cu into oxide form in this process is possible, providing that a relatively high dosage of steam is passed through the reactor.

b) The highest recovery of copper was found for oxidative smelting of the PY sample (89.6% of Cu), then for reductive smelting of the IN sample (67.2% of Cu). Intensive transport of metals between metallic and slag phases is necessary for coalescence and separation of the metallic phase.

c) Significant differences between the relative recovery of precious metals (towards Cu) results from the level of oxygen potential. It was found that in the case of gold, high oxygen potential is beneficial for its recovery, oppositely than for silver.

d) The remaining metals (Fe, Ni, and non-ferrous metals) recovery is correlated with Cu recovery, but only in a reductive atmosphere, especially for RE/SG (dominant) and RE/PY (considerable) processes. The presence of Fe and Ni enables the separation of the metallic magnetic fraction composed of non-ferrous elements and copper (of high mass contribution).

Two-stage thermal processing involving the elimination of the organic phase in the first stage (also, the elimination of the use of air - PY and GS) and smelting in the second one should be developed as an alternative for the traditional one-stage process, dominating nowadays in the industrial pyrometallurgical technologies. However, the efficiency of copper and precious metals (Au, Ag, Pd) recovery by further metallurgical smelting requires careful optimization involving in the first place investigations of the intensity of metal transport through the metal/slag interface.

### Acknowledgments

We thank Anna Szymczycha-Madeja for some analytical measurements. The work was financed by statutory activity subsidies from the Polish Ministry of Science and Higher Education for the Faculty of Environmental Engineering and Faculty of Chemistry of Wrocław University of Science and Technology.

### References

- ARSHADI, M.; YAGHMAEI, S.; MOUSAVI, S. M., 2018. *Study of plastics elimination in bioleaching of electronic waste using Acidithiobacillus ferrooxidans*. Int. J. Environ. Sci. Technol. 16, 7113–7126. <https://doi.org/10.1007/s13762-018-2120-1>
- BALDÉ, C. P.; FORTI, V.; GRAY, V.; KUEHR, R.; STEGMANN, P., 2017. *The Global E-waste Monitor 2017: Quantities, Flows, and Resources*. International Telecommunication Union (ITU) & International Solid Waste Association (ISWA), Bonn/Geneva/Vienna, ISBN 978-92-808-9054-9
- BAZARGAN, A.; BWEGENDAHO, D.; BARFORD, J.; MCKAY, G., 2014. *Printed circuit board waste as a source for high purity porous silica*. Sep. Purif. Technol. 136, 88–93.
- BELLEMANS, I.; DEWILDE, E.; MOELANS, N.; VERBEKEN, K., 2018. *Metal losses in pyrometallurgical operations - A review*. Adv. Colloid Interface Sci. 255, 47–63.
- CAYUMIL, R.; KHANNA, R.; RAJARAO, R.; MUKHERJEE, P.S.; SAHAJWALLA, V., 2016. *Concentration of precious metals during their recovery from electronic waste*. Waste Manage. 57, 121–130.
- CUCCHIELLA, F.; D'ADAMO, I.; KOH, S.C.L.; ROSA, P., 2015. *Recycling of WEEEs: An economic assessment of present and future e-waste streams*. Renew. Sust. Energ. Rev. 51, 263–272.
- CUI, J.; ZHANG, L., 2008. *Metallurgical recovery of metals from electronic waste: A review*, J. Hazard. Mater. 158, 228–256.
- de ANDRADE, L.M.; ROSARIO, C.G.A.; DE CARVALHO, M.A., 2019. *Copper Recovery from Printed Circuit Boards from Smartphones Through Bioleaching*, In: TMS 2019 148th Annual Meeting & Exhibition Supplemental Proceedings. The Minerals, Metals & Materials Series, Eds; Springer: Cham, Switzerland, 837–844.
- DÍAZ-MARTÍNEZ, M.E.; ARGUMEDO-DELIRA, R.; SÁNCHEZ-VIVEROS, G.; ALARCÓN, A.; MENDOZA-LÓPEZ, M.R., 2019. *Microbial Bioleaching of Ag, Au and Cu from Printed Circuit Boards of Mobile Phones*. Curr. Microbiol. 76, 536–544.
- ELSHKAKI, A.; GRAEDEL, T.E.; CIACCI, L.; RECK, B.K., 2018. *Resource Demand Scenarios for the Major Metals*. Environ. Sci. Technol. 52, 2491–2497.
- FEDERICO, L.M.; CHIDIAC, S.E., 2009. *Waste glass as a supplementary cementitious material in concrete – Critical review of treatment methods*. Cement Concrete Comp. 31(8), 606–610.
- FORTI, V.; BALDE, C.P.; KUEHR, R., 2018. *E-waste statistic: Guidelines on classification, reporting and indicators, 2nd ed.*. United Nations University: Bonn, Germany, ISBN 978-92-808-9067-9
- GURGUL, A.; SZCZEPANIAK, W.; ZABŁOCKA-MALICKA, M., 2018. *Incineration and pyrolysis vs. steam gasification of electronic waste*. Sci. Total Environ. 624, 1119–1124.
- HSC Chemistry® Ver. 6.12, Outotec (Finland) Oy.

- IANNICELLI-ZUBIANI, E. M.; GIANI, M. I.; RECANATI, F.; DOTELLI, G.; PURICELLI, S.; Cristiani, C., 2017. *Environmental impacts of a hydrometallurgical process for electronic waste treatment: A life cycle assessment case study*. J. Clean. Prod. 140 (3), 1204–1216.
- IŞILDAR, A.; RENE, E. R.; VAN HULLEBUSCHA, E. D.; LENS, P.N.L., 2018. *Electronic waste as a secondary source of critical metals: Management and recovery technologies*. Resour. Conserv. Recycl. 135, 296–312.
- KAYA, M., 2016. *Recovery of metals and nonmetals from electronic waste by physical and chemical recycling processes*. Waste Manage. 57, 64–90.
- KAYA M., 2017. *Recovery of Metals and Nonmetals from Waste Printed Circuit Boards (PCBs) by Physical Recycling Techniques*. In: Energy Technology 2017. The Minerals, Metals & Materials Series. Zhang, L., Drelich, J. W., Neelameggham, N. R., Guillen, D. P., Haque, N., Zhu, J., Sun, Z., Wang, T., Howarter, J. A., Tesfaye, F., Ikhmayies, S., Olivetti, E., Kennedy, M. W., Eds; Springer: Cham, Switzerland, 433–451.
- KHALIQ, A.; RHAMDHANI, M. A.; BROOKS, G.; MASOOD, S., 2014. *Metal Extraction Processes for Electronic Waste and Existing Industrial Routes: A Review and Australian Perspective*. Resources 3(1) 152–179.
- KUMARI, A.; JHA, M.K.; LEE, J.; SINGH, R. P., 2016 a. *Clean process for recovery of metals and recycling of acid from the leach liquor of PCBs*. J. Clean. Prod. 112 (5), 4826–4834.
- KUMARI, A.; JHA, M. K.; SINGH, R. P., 2016 b. *Recovery of metals from pyrolysed PCBs by hydrometallurgical techniques*. Hydrometallurgy, 165 (1), 97–105.
- MAN, M.; NAIDU, R.; WONG, M. H., 2013. *Persistent toxic substances released from uncontrolled e-waste recycling and actions for the future*. Sci Total Environ. 463–464, 1133–1137.
- NAVAZO, J.M.V.; MÉNDEZ, G.V.; PEIRÓ, L.T., 2014. *Material flow analysis and energy requirements of mobile phone material recovery processes*. Int. J. Life Cycle Assess. 19, 567–579.
- PANT, D.; JOSHI, D.; UPRETI, M.K.; KOTNALA, R.K., 2012. *Chemical and biological extraction of metals present in E waste: A hybrid technology*. Waste Manage. 32(5), 979–990.
- PICKLES, C.A.; HARRIS, C.; PEACEY, J., 2011. *Silver loss during the oxidative refining of silver-copper alloys*. Miner. Eng. 2011, 24, 514–523.
- PRIYA, A.; HAIT, S., 2017. *Comparative assessment of metallurgical recovery of metals from electronic waste with special emphasis on bioleaching*. Environ. Sci. Pollut. Res. 24(8), 6989–7008. <https://doi.org/10.1007/s11356-016-8313-6>
- SCHIPPER, B. W.; LIN, H. C.; MELONI, M. A.; WANSLEEBEN, K.; HEIJUNGS, R.; DER VOETA, E., 2018. *Estimating global copper demand until 2100 with regression and stock dynamics*. Resour. Conserv. Recycl. 132, 28–36.
- SETHURAJAN, M.; VAN HULLEBUSCH, E. D.; FONTANA, D.; AKCIL, A.; DEVECI, H.; BATINIC, B.; LEAL, J. P.; GASCHÉ, T.A.; KUCUKER, M. A.; KUCHTA, K.; NETO, I. F. F.; SOARES, H.; CHMIELARZ, A., 2019. *Recent advances on hydrometallurgical recovery of critical and precious elements from end of life electronic wastes - a review*. Crit. Rev. Environ. Sci. Technol. 49(3), 212–275.
- SHUVA, M.A.H.; RHAMDHANI, M.A.; BROOKS, G.A.; MASOOD, S.; REUTER, M.A., 2016. *Thermodynamics data of valuable elements relevant to e-waste processing through primary and secondary copper production: a review*. J. Clean. Prod. 131, 795–809.
- SZCZEPANIAK, W., ZABŁOCKA-MALICKA, M., GURGUL, A., OCHROMOWICZ, K., 2020. *Acidic leaching of steam gasified, pyrolyzed and incinerated PCB waste from LCD screen*, Physicochem. Probl. Miner. Process. 56, 257–268.
- THE INTERNATIONAL CENTRE FOR DIFFRACTION DATA, PDF-2 Database, 12 Campus Blvd., Newtown Square, PA 19073-3273 U.S.A, 1998.
- VENTURA, E.; FUTURO, A.; PINHO, S.C.; ALMEIDA, M.F.; DIAS, J.M., 2018. *Physical and thermal processing of Waste Printed Circuit Boards aiming for the recovery of gold and copper*. J Environ. Manage. 223, 297–305.
- WANG, H.; ZHANG, S.; LI, B.; PAN, D.; WU, Y.; ZUO, T., 2017. *Recovery of waste printed circuit boards through pyrometallurgical processing: A review*. Resour. Conserv. Recycl. 126, 209–218.
- YAMAGUCHI, K., 2018. *Thermodynamic Study of the Equilibrium Distribution of Platinum Group Metals Between Slag and Molten Metals and Slag and Copper Matte*. In: Extraction 2018, The Minerals, Metals & Materials Series Davis, B. R., Moats, M. S., Wang, S. Eds.; Springer: Cham, Switzerland, 797–804.
- ZABŁOCKA-MALICKA, M.; RUTKOWSKI, P.; SZCZEPANIAK, W., 2015. *Recovery of copper from PVC multiwire cable waste by steam gasification*. Waste Manage. 2015, 46, 488–496.
- ZABŁOCKA-MALICKA, M.; SZCZEPANIAK, W.; RUTKOWSKI, P.; OCHROMOWICZ, K.; LEŚNIEWICZ, A.; CHEĆMANOWSKI, J., 2018. *Decomposition of the ISA-card under steam for valorized polymetallic raw material*. J. Anal. Appl. Pyrolysis. 130, 256–268.

- ZHANG, Y.; LIU, S.; XIE, H.; ZENG, X.; LI, J., 2012 a. *Current status on leaching precious metals from waste printed circuit boards*. *Procedia. Environ. Sci.* 16, 560-568.
- ZHANG, Z.; XIAO, Y.; VONCKEN, J.; YANG, Y.; BOOM, R.; WANG, W.; ZOU, Z., 2012 b. *Thermodynamic assessment of the CaO-Na<sub>2</sub>O-SiO<sub>2</sub> slag system*. In *Ninth International Conference on Molten Slags, Fluxes and Salts. Proceedings of the Molten 2012, Beijing, China, May 27-30th, Extended Abstracts* p. 40.
- ZHANG, L.; XU, Z., 2016. *A review of current progress of recycling technologies for metals from waste electrical and electronic equipment*. *J. Clean. Prod.* 127 19-36.